

22nd Machining Innovations Conference for Aerospace Industry 2022 (MIC 2022),
November 30th and December 1st 2022, Hannover, Germany

Influence of hybrid-additive interfaces manufactured by laser powder bed fusion on the surface topography after machining of Ti-6Al-4V

Patrick Fischmann^{a,*}, Volker Schulze^a, Frederik Zanger^a

^a*Institute of Production Science (wbk), Karlsruhe Institute of Technology (KIT), Kaiserstraße 12, 76131 Karlsruhe*

* Corresponding author. Tel.: +49 174 330 2753; fax: +49 721 608-45004; E-mail address: patrick.fischmann@kit.edu

Abstract

In hybrid-additive manufacturing, additive structures are produced on wrought base bodies. Hybrid-additive manufacturing using Powder Bed Fusion - Laser Beam offers unrestricted freedom of design with reduced build time and thus more economical production. Between the wrought and additive component area, an interface is created which has different microstructural properties. In this paper, the influence of the hybrid-additive interface on the machining process and its resulting surface topography is investigated. For this purpose, hybrid-additive specimens (Ti-6Al-4V on Ti-6Al-4V) are manufactured in as-built condition and after heat treatment (4 h at 800 °C). The specimens are machined by circumferential climb milling. For detailed investigation, the tests are carried out with a single-tooth tool at varying cutting speeds and depth of cut. Micrographs show a hardly existent heat affected zone in the interface. The additive microstructure shows higher hardness than the wrought microstructure, the delta is reduced with heat treatment. The delta in hardness leads to different cutting forces which in turn result in differing tool deflection. Hence, waviness W_t between the microstructure are observed depending on control variables. High cutting speeds and high depth of cut result in the lowest waviness of 4.2 μm . Further, heat treatment reduces the scatter of roughness values in additive microstructure.

© 2022 The Authors. Published by SSRN, available online at <https://www.ssrn.com/link/MIC-2022.html>

This is an open access article under the CC BY-NC-ND license (<http://creativecommons.org/licenses/by-nc-nd/4.0/>)

Peer review statement: Peer-review under responsibility of the scientific committee of the 22nd Machining Innovations Conference for Aerospace Industry 2022

Keywords: Selective laser melting; hybrid additive manufacturing; cutting force; surface topography; Ti-6Al-4V

1. Introduction

Powder bed-based additive manufacturing (PBF-LB) enables the production of complex geometries. Bionic structures with complex free-form surfaces used in lightweight construction can be produced by this method. In the aerospace sector, Ti-6Al-4V is used due to its low density, high strength and good corrosion resistance [1]. Additive manufacturing enables functional integration through internal structures, for example cooling channels [2]. However, the process of iteratively applying powder and melting it locally using a laser is time-consuming. Economical production through conventional process chains, e.g. casting and machining, is usually not possible due to the complex geometry. The new

hybrid-additive manufacturing leads to reduced build-up times in additive manufacturing [3] and still enables complex geometries [4]. In this method, the additive manufacturing process is carried out on a large-volume, conventionally manufactured base body. High surface roughness in the PBF-LB process leads to insufficient fatigue strength in the additive part [5]. In addition, possible cracks between the additive structure and the base body occur [6] which can initiate failure. The influence of both on the fatigue strength can be reduced by post-machining.

Hybrid-additive manufacturing is receiving a great amount of attention in research, independently of the material. In the context of this work, current research work on the material Ti-6Al-4V will be dealt with in the following. The production of

© 2022 The Authors. Published by SSRN, available online at <https://www.ssrn.com/link/MIC-2022.html>

This is an open access article under the CC BY-NC-ND license (<http://creativecommons.org/licenses/by-nc-nd/4.0/>)

Peer review statement: Peer-review under responsibility of the scientific committee of the 22nd Machining Innovations Conference for Aerospace Industry 2022.

hybrid sheet metal structures, in which additive manufacturing is performed on thin sheet metals, was investigated in the work of Bhrigu et al. [6] and Huber et al. [7]. Micrographs of the interface showed cracks on the outside of the component in the interface after hybrid-additive manufacturing of cylinders on sheet metal. This can be reduced by using suitable radii in the transition zone, which also increases the shear strength [6]. When varying the energy density in the hybrid-additive process, Huber et al. observed an influence on the microstructure in the interface. The increase of the volume energy density from 46.3 to 222.2 J/mm³ led to a pronounced heat affected zone (HAZ) [7]. This HAZ is also observed in the work of Neuenfeldt et al. [8] at a volume energy density of 44.2 J/mm³ during additive manufacturing. The HAZ has a higher hardness than the wrought and additive microstructure. Also manufacturing with powder-based directed energy deposition leads to a HAZ with increased hardness [9]. Dolev et al. [10] did not determine an increased hardness in the transition between wrought and additive microstructure. A correlation with the energy density is not possible due to the lack of information on the layer thickness.

Ti-6Al-4V is considered a difficult material to machine due to its high strength and low thermal conductivity [1]. The effect of process parameters on cutting forces and surface properties has been extensively studied [11]. Increasing cutting speed leads to lower cutting forces; from cutting speeds $v_c > 200$ m/min the cutting force increases again. The value of the roughness develops analogously with a minimum at 200 m/min [12]. Yang & Liu [13] showed low roughness at high cutting speeds (maximum 110 m/min), low radial depth of cut a_e and feed rate f_z . The changed microstructural properties in additive manufacturing compared to conventionally manufactured Ti-6Al-4V result in larger chip forces, the chip morphologies are similar to those of conventional Ti-6Al-4V [14]. Milton et al. [15] measured higher axial forces in additively manufactured specimens, but found only small microstructural changes between the microstructures. Lizzul et al. [16] observed increasing roughness with additive microstructure at higher cutting speed and feed rate. It is only Neuenfeldt et al. [8] that considers the cutting of the interface of hybrid-additive specimens. Due to the HAZ with increased hardness described in the previous section, the specimens show a peak in roughness after an orthogonal cut. The effect is reduced with a previously conducted heat treatment.

In this work, the influence of the interface of hybrid additive manufactured samples of Ti-6Al-4V on the cutting forces during machining and the resulting surface properties is investigated. The aim is to achieve low roughness and waviness of the machined surface.

2. Materials and Methods

2.1. Specimens Manufacturing

In order to investigate the influence of the microstructure or its combination, three types of specimens were produced. The purely conventional specimens were only prepared by

machining the desired geometry. The base material was used in a hot rolled and annealed (705 °C 1 h + air cooling) state according to ASTM F136-13. The material was also used for the base of the hybrid-additive specimens. For the hybrid-additive production, a M4 thread and two 4H7 stake out bores were manufactured in the conventional base bodies. With these, the components could be clamped onto a specially prepared build platform. The arithmetic roughness R_a of the prepared base bodies was $< 1 \mu\text{m}$. Three build jobs were necessary for the production of the specimens; the specimens were sorted according to size so that the components in the respective build job had a height deviation of < 0.01 mm. The additive manufacturing of the build-ups with a height of 6 mm was carried out on an eos M290 with a spot diameter of 44.58 μm at 200 W. The used Ti-6Al-4V powder from eos GmbH (Krailling) has a chemical composition according to ISO 5832-3, ASTM F1472 and ASTM B348. The components were manufactured with the following parameters: laser power 340 W, scan speed 1250 mm/s, hatch distance 0.12 mm and layer thickness 0.06 mm. The volume energy density with the mentioned process parameters is 37.8 J/mm³. The first three layers (0.00 mm, 0.06 mm, 0.12 mm) were exposed twice. Stripe filling with a stripe length of 5 mm and a rotation of 67° per layer was used as the scanning strategy. The build platform was preheated to 80 °C. The parameters mentioned were also used for the purely additive specimens. These were fabricated directly onto a Ti-6Al-4V build platform. After fabrication, the specimens were eroded off and half of each specimen type was heat treated at 800 °C for 4 h in an argon atmosphere and furnace cooling.

2.2. Experimental procedure

The finishing by means of circumferential milling was carried out on a Heller MC16 machining center. In addition to the conventionally, additively and hybrid-additively manufactured specimens, the control variables cutting speed v_c (60 and 100 m/min) and radial depth of cut a_e (0.2 and 1.0 mm) were varied full factorial. Each test was carried out three times. In order to exclude wear effects on the tool, the milling tool was changed after each test series. The axial depth of cut a_p was constant 12 mm during the tests, the feed per tooth f_z was 0.1 mm. The tests were carried out with the DHC INOX Premium end mill from LMT Tools (Schwarzenbek) with a diameter of 12 mm. The cuts were performed in climb milling to avoid friction and squeezing phases at cutting edge entry. Due to the high thermal load on the cutting edges, milling was carried out with flood cooling [1]. The used coolant was Jokisch HPC VEG high-performance cooling lubricant with a concentration of 7 %. A precut was carried out before the measurement. This eliminates unintended geometric deviations and effects caused by the additive surface layer. An overview of all tests is provided in table 1.

During machining, the cutting forces were recorded with a force measuring platform (Kistler Type Z10440) and three charge amplifiers (Kistler Charge Meter Type 5015), one for each force. To reduce the excitation frequency of the

measurement setup and thus increase the measurement quality, the tests were carried out with a special single-tooth tool. The individual forces in the x-, y- and z-directions (Fig. 1, a) were recorded at a data rate of 10 kHz. The force measurement was evaluated with Matlab. Run-in and run-out effects of the tool were not considered. By means of a time-synchronous signal average (tsa), the cutting forces recorded per revolution were averaged, see Fig. 1, b). In the exemplary force profile (hybrid-additive part without heat treatment), the areas cutting edge entry, constant chip formation and cutting edge exit are indicated. During the latter two areas, the formation of the final surface takes place. Within the constant chip formation, the cutting edge of a hybrid-additive part changes from a wrought to an additive microstructure. For the evaluation of the cutting forces, the maxima of the force at the beginning in the wrought as well as in the additive area are used.

After machining, the roughness of each specimen was measured. This was done tactilely and optically as explained in Fig. 2. The roughness R_z of the individual areas conventionally and additively was measured parallel to the feed direction with

Table 1. Experimental overview.

Control variables	
Manufacturing method	Wrought/Additive/Hybrid-additive
Heat treatment	as-built/800 °C 4 h
Cutting speed v_c in m/min	60/100
Radial depth of cut a_e in mm	0.2/1.0
Constant Control variables	
Axial depth of cut a_p in mm	12
Feed per tooth f_z in mm/rev	0.1

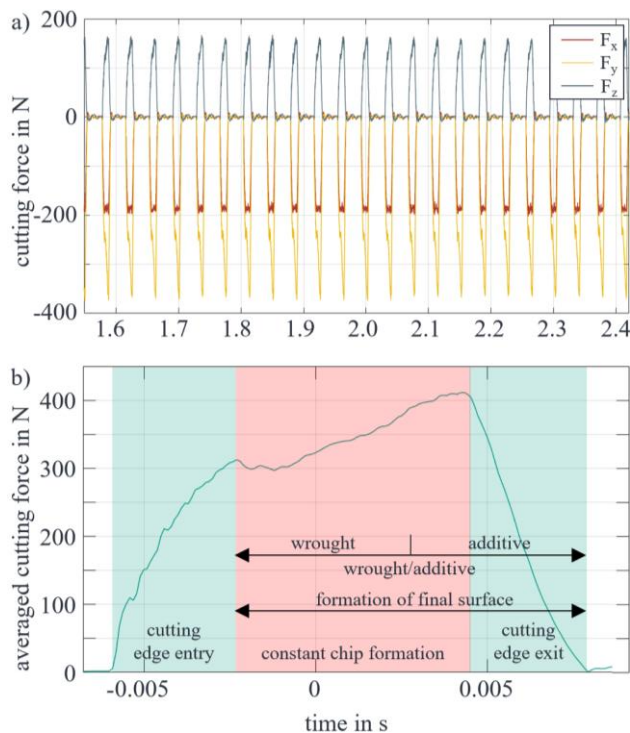


Fig. 1. Cutting force measurement. a) cutting force in N in x-, y- and z direction. b) absolute averaged cutting force in N in x- and y-direction with cutting condition.

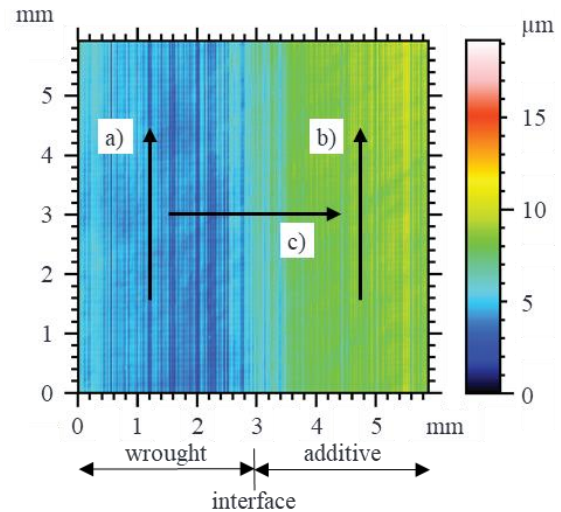


Fig. 2. Surfaces roughness measurement of hybrid-additive part. a) tactile, parallel to feed direction, wrought. b) tactile, parallel to feed direction, additive. c) optical, orthogonal to feed direction, interface.

optical measurement (μ surf, NanoFocus AG, Oberhausen) was carried out orthogonally across the interface. Starting in the wrought area, this enables the determination of the maximum waviness W_t between the individual areas.

For microstructural analyses, three hybrid-additive specimens with and without heat treatment were embedded, ground and polished. To activate the surface, the final polishing step was performed with a solution of 80 % OPS and 20 % hydrogen peroxide. The etching was performed according to Weck [17] for 40 seconds. The micrographs were taken on the ZEISS AxioScope 5 light microscope (LM), a deeper look in the interface was performed by scanning electron microscopy (SEM) using the JEOL JSM-6010 LV.

The micrograph was followed by the hardness measurement of the individual microstructures. The Vickers hardness test HV0.1 was carried out according to DIN EN ISO 6507-1 on a Falcon 600 (Innovatest Deutschland GmbH, Selkant-Heilder). In each case seven measuring points with a distance of 0.2 mm were placed symmetrically to the interface. Thus, three measuring points are located in the wrought area, the central point exactly on the interface and three points in the additive microstructure. This series of measurements is supplemented by measuring points symmetrical to the interface at a distance of 3 mm each.

3. Results

3.1. Microstructural analysis and hardness

Ti-6Al-4V forms a two-phase structure of α - and β -titanium during cooling. The α -phase has an hcp lattice structure while the β -phase forms a bcc lattice structure. At near-equilibrium cooling, α -nuclei form at the β -grain boundaries [18]. At sufficiently high cooling rates, diffusion is suppressed and a pure martensitic structure of acicular α' -phase forms [19]. Fig. 3 shows light microscopic images of hybrid-additive manufactured specimens. In the additive region without heat

treatment, the acicular α' -martensite can be seen. This is due to high cooling rates in PBF-LB. The wrought microstructure shows a preferred orientation with globular grains. Between the first meltpool boundaries and the wrought part, the microstructure shows a tiny HAZ. The two microstructures are approximated by the heat treatment. Since the heat treatment takes place below the β -transus temperature, no complete recrystallization takes place.

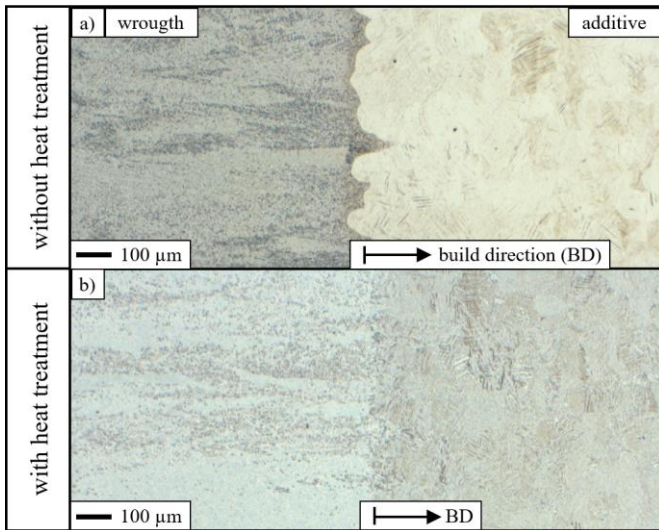


Fig. 3. LM microsections of interface of hybrid-additive specimens, a) without heat treatment and b) with heat treatment (800 °C 4 h)

A detailed examination of the interface is shown in the SEM images in Fig. 4. Fig. 4 a) and b) again show the hybrid-additive specimens without heat treatment. The acicular martensite is predominantly oriented parallel to the build-up direction. A duplex microstructure of acicular α' -martensite and globular microstructure can be seen. The globular structure consists of α -plates with β -phase at the grain boundaries. Due to the heat treatment, the martensitic α' -structure transforms into a mixed structure of α and β , see Fig. 4 c) and d). The microstructure remains acicular. A distinct HAZ as shown in [7] and [8] could not be detected.

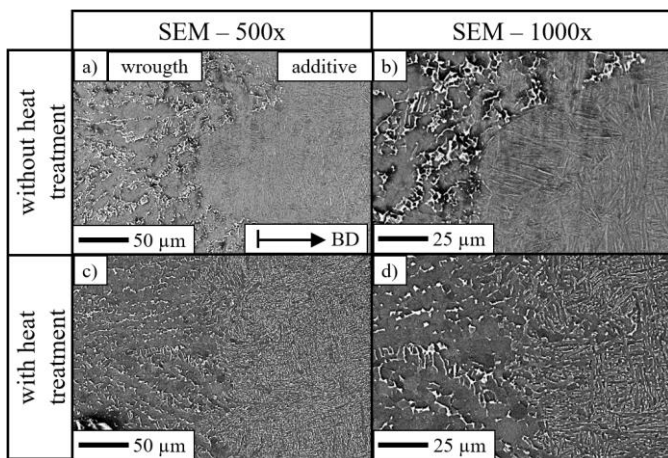


Fig. 4. SEM microsections of the interface of hybrid-additive specimens. a) and b) without heat treatment. c) and d) with heat treatment (800 °C 4 h)

Fig. 5 shows the hardness profiles of the hybrid-additive manufactured specimens. Error bars indicate the scatter of measured values. Before heat treatment, the additive area shows a Vickers hardness of 457 HV0.1, the value decreases in the interface to 384 HV0.1. The conventional microstructure shows a minimum of 321 HV0.1 near the interface and increases with increasing distance to 349 HV0.1. Due to the heat treatment and the described microstructure transformation, the hardness is reduced. In the additive range the hardness is reduced by 16.5 % to 392 HV0.1. This effect decreases in the interface zone. The hardness of the conventional area is also reduced by the heat treatment; the decrease here is 11 %.

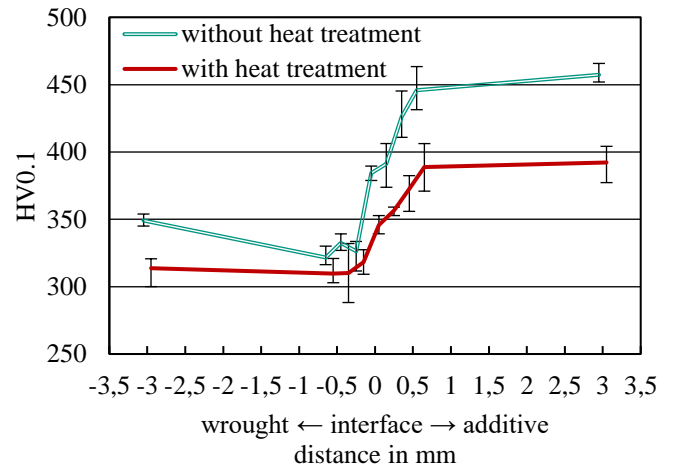


Fig. 5. Vickers hardness HV0.1 in hybrid-additive specimens

The reduction in hardness in the conventional section results from the increased temperature and duration of the heat treatment. The starting material was annealed at 705 °C for 1 h while the heat treatment after the additive build-up was carried out at 800 °C for 4 h. Hence, further structural transformations took place

3.2. Surface roughness and waviness

The average roughness R_z shows varying effects depending on the manufacturing method and the heat treatment. R_z is between 0.4 and 1.0 μm for the wrought microstructure and the additive microstructure, respectively.

Fig. 6 shows the roughness of the respective conventional zone of the purely conventional and hybrid-additive specimens. In the following plots, error bars indicate the scatter (min./max. values) of measured values. The mean values of the roughness R_z are comparable depending on the cutting speed. Also, the values do not show constant effects between the heat treatment conditions. Furthermore, the scatter of measured values does not show any pattern depending on the control variables. Statements based on minor deviations of the averaged roughness values between wrought parts and the wrought area of hybrid-additive parts are affected by overlapping error bars. Consequently, in the conventional range, no justified systematics between roughnesses, heat treatment conditions and control variables is possible during circumferential milling.

Fig. 7 shows the roughness of the respective additive zones of purely additive and hybrid-additive specimens. The purely additive specimens show an increased roughness compared to the additive structure of the hybrid-additive specimens. This effect is more pronounced for specimens without heat treatment, only at $v_c = 60$ m/min und $a_e = 0.2$ mm the effect is contrary. In addition to the increase in the mean value, the scattering of the values increases by a factor of 2 - 4. The roughness difference between the pure additive and hybrid-additive specimens may result from the thermal history of the samples. The height and thus the energy introduced is not the same for the cutting zone in the component, which may result in minor microstructural changes.

Fig. 8 shows the maximum waviness W_t of the hybrid-additive specimens as a function of the control variables during circumferential milling. The results show varying effects depending on the cutting speed. At low cutting speeds, the waviness and the scatter of the values are greater. In addition, the waviness is 22 and 51 % higher at greater radial cutting depths. The maximum averaged value is 13.51 μm , at this high value geometrical tolerances may be exceeded. At low radial depth of cut, the waviness between the cutting speeds is comparable, but decreases slightly. Especially for specimens without heat treatment, the scatter of the measured data is reduced. A high cutting speed and a high radial depth of cut result in the lowest waviness, which is only 4.2 μm for heat treated specimens.

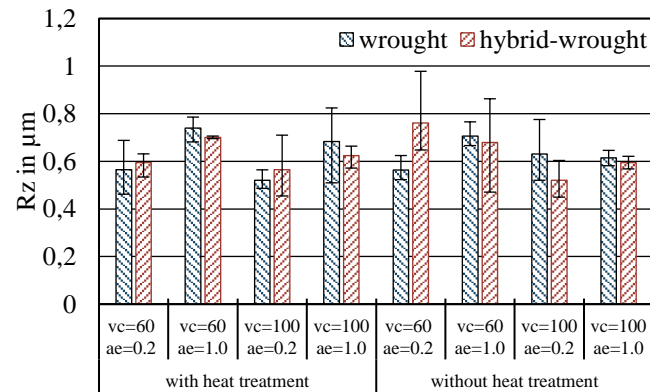


Fig. 6. Averaged roughness R_z of wrought specimens and the wrought part of hybrid-additive specimens

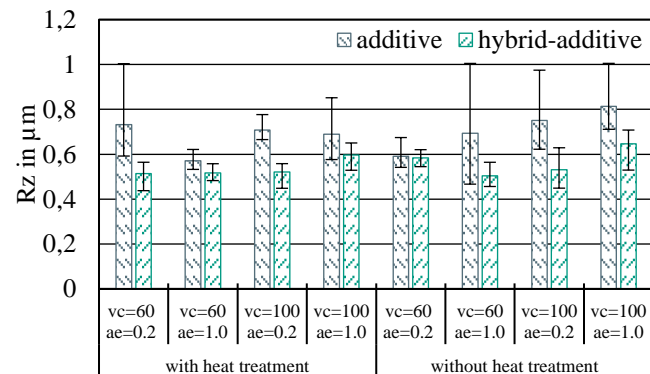


Fig. 7. Averaged roughness R_z of additive specimens and the additive part of hybrid-additive specimens

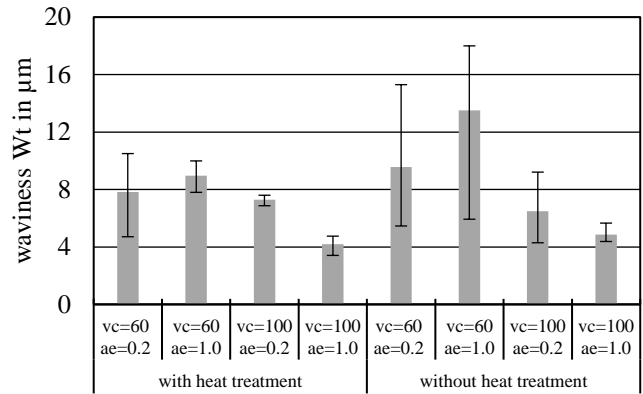


Fig. 8. Waviness W_t in hybrid-additive specimens, measured orthogonal to the interface

3.3. Correlation of cutting force on waviness

Fig. 9 shows the absolute cutting force of hybrid-additive manufactured specimens. At low radial depth of cut $a_e = 0.2$ mm, the cutting force average is 108 N with values between 90 and 145 N. At high a_e (1 mm), the averaged value is 337 N (283-411 N). The increase in a_e results in an increase of the maximum chip thickness from 12.9 to 28.9 μm . The increase in averaged cutting force (factor 3.1) is higher compared to the increase in maximum chip thickness (factor 2.2). Further, the delta in hardness between the additive and the wrought part is 107 HV0.1 without heat treatment and 75.5 HV0.1 with heat treatment. The reduction of 6 % results in the lower force delta between the microstructures observed at higher depth of cut. In general, higher depth of cut results in a higher cutting force delta between the areas of the hybrid-additive manufactured parts compared to low depths of cut. The higher cutting force leads to increasing deflection of the tool this effect is pronounced at specimens without heat treatment. Due to this, the waviness is higher at as-built specimens. The effect is reduced at heat treated parts.

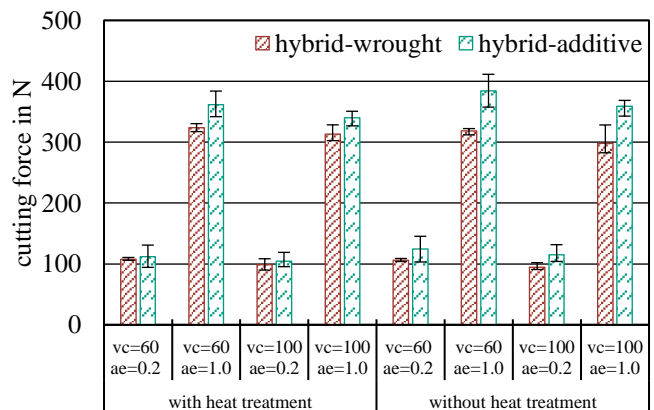


Fig. 9. Absolute cutting force in x- and y-direction on workpiece

4. Conclusion

In this work, the effect of the interface of hybrid-additive manufactured specimens of Ti-6Al-4V on the cutting forces during machining and the resulting surface properties was investigated. The microstructure, hardness, cutting force, surface roughness and waviness were considered with the following results:

- In the manufactured hybrid-additive parts the heat affected zone is hardly existent. Hardness in the interface does not exceed the hardness of the additive part but is higher than in the wrought part.
- Averaged value and scatter of roughness R_z in the additive part of hybrid-additive specimens is reduced compared to purely additively manufactured parts.
- The higher waviness in hybrid-additive specimens occurs due to deflection of the tool. This is due to higher cutting forces caused by the higher hardness of the additive microstructure. For components without heat treatment and high depth of cut and feed, the shape tolerances may not be fulfilled due to large waviness. With heat treatment before machining, waviness of hybrid-additive parts is reduced.

Acknowledgements

This paper is funded by “MeSATech” as part of the “ProMed” BMBF project (funding reference number: 02P18C135) supervised by the Project Management Agency Karlsruhe (PTKA).

The authors thank FIT AG for manufacturing the additive and hybrid-additive parts. Furthermore, the authors would like to thank Aesculap for the heat treatment of the specimens and LMT Tools for providing the cutting tools.

References

- [1] Klocke, F. (2018). *Fertigungsverfahren 1: Zerspanung mit geometrisch bestimmter Schneide*. Springer-Verlag.
- [2] Liu, R., Wang, Z., Sparks, T., Liou, F., & Newkirk, J. (2017). Aerospace applications of laser additive manufacturing. In *Laser additive manufacturing* (pp. 351-371). Woodhead Publishing.
- [3] Eschner, N., Kopf, R., Lieneke, T., Künneke, T., Berger, D., Häfner, B., ... & Zimmer, D. (2017). Kombination etablierter und additiver Fertigung. *Zeitschrift für wirtschaftlichen Fabrikbetrieb*, 112(7-8), 469-472.
- [4] Meiners, F., Ihne, J., Jürgens, P., Hemes, S., Mathes, M., Sizova, I., ... & Weisheit, A. (2020). New hybrid manufacturing routes combining forging and additive manufacturing to efficiently produce high performance components from Ti-6Al-4V. *Procedia Manufacturing*, 47, 261-267.
- [5] Murakami, Y., Masuo, H., Tanaka, Y., & Nakatani, M. (2019). Defect analysis for additively manufactured materials in fatigue from the viewpoint of quality control and statistics of extremes. *Procedia Structural Integrity*, 19, 113-122.
- [6] Ahuja, B., Schaub, A., Karg, M., Schmidt, R., Merklein, M., & Schmidt, M. (2015, March). High power laser beam melting of Ti-6Al-4V on formed sheet metal to achieve hybrid structures. In *Laser 3D Manufacturing II* (Vol. 9353, pp. 118-127). SPIE.
- [7] Huber, F., Papke, T., Kerken, M., Tost, F., Geyer, G., Merklein, M., & Schmidt, M. (2019). Customized exposure strategies for manufacturing hybrid parts by combining laser beam melting and sheet metal forming. *Journal of Laser Applications*, 31(2), 022318.
- [8] Neuenfeldt, M., Zanger, F., & Schulze, V. (2020). Machining of Hybrid (Conventionally and Additively) built 316L, IN718 and Ti-6Al-4V Specimen. *HTM Journal of Heat Treatment and Materials*, 75(3), 192-203.
- [9] Ma, J., Zhang, Y., Li, J., Cui, D., Wang, Z., & Wang, J. (2021). Microstructure and mechanical properties of forging-additive hybrid manufactured Ti-6Al-4V alloys. *Materials Science and Engineering: A*, 811, 140984.
- [10] Dolev, O., Osovski, S., & Shirizly, A. (2021). Ti-6Al-4V hybrid structure mechanical properties—Wrought and additive manufactured powder-bed material. *Additive Manufacturing*, 37, 101657.
- [11] Niknam, S. A., Khettabi, R., & Songmene, V. (2014). Machinability and machining of titanium alloys: a review. *Machining of titanium alloys*, 1-30.
- [12] Wang, F., Zhao, J., Li, A., & Zhao, J. (2014). Experimental study on cutting forces and surface integrity in high-speed side milling of Ti-6Al-4V titanium alloy. *Machining Science and Technology*, 18(3), 448-463.
- [13] Yang, D., & Liu, Z. (2015). Surface topography analysis and cutting parameters optimization for peripheral milling titanium alloy Ti-6Al-4V. *International Journal of Refractory Metals and Hard Materials*, 51, 192-200.
- [14] Le Coz, G., Fischer, M., Piquard, R., D’acunto, A., Laheurte, P., & Dudzinski, D. (2017). Micro cutting of Ti-6Al-4V parts produced by SLM process. *Procedia Cirp*, 58, 228-232.
- [15] Milton, S., Morandea, A., Chalon, F., & Leroy, R. (2016). Influence of finish machining on the surface integrity of Ti6Al4V produced by selective laser melting. *Procedia Cirp*, 45, 127-130.
- [16] Lizzul, L., Sorgato, M., Bertolini, R., Ghiotti, A., & Bruschi, S. (2021). Anisotropy effect of additively manufactured Ti6Al4V titanium alloy on surface quality after milling. *Precision Engineering*, 67, 301-310.
- [17] Weck, E., & Leistner, E. (Eds.). (1986). *Metallographische Anleitung zum Farbätzen nach dem Tauchverfahren: Metallographic instructions for colour etching by immersion. Nichteisenmetalle, Hartmetalle und Eisenwerkstoffe, Nickel-Basis- und Kobalt-Basis-Legierungen. Non-ferrous metals, cemented carbides and ferrous metals, nickel-base and cobalt base alloys*. Deutscher Verlag für Schweißtechnik.
- [18] Scharowsky, T. (2017). *Grundlagenuntersuchungen zum selektiven Elektronenstrahlschmelzen von TiAl6V4*. FAU University Press.
- [19] Ahmed, T., & Rack, H. J. (1998). Phase transformations during cooling in $\alpha + \beta$ titanium alloys. *Materials Science and Engineering: A*, 243(1-2), 206-211.